



ZEEMAN DOPPLER MAPS: ALWAYS UNIQUE, NEVER SPURIOUS?

MARTIN J. STIFT^{1,2} AND FRANCESCO LEONE^{1,2}

¹ Armagh Observatory, College Hill, Armagh BT61 9DG, UK

² Università degli Studi di Catania, Osservatorio Astrofisico di Catania, via S. Sofia 78, I-95123 Catania, Italy
Received 2016 June 13; revised 2016 October 25; accepted 2016 October 25; published 2016 December 27

ABSTRACT

Numerical models of atomic diffusion in magnetic atmospheres of ApBp stars predict abundance structures that differ from the empirical maps derived with (Zeeman) Doppler mapping (ZDM). An in-depth analysis of this apparent disagreement investigates the detectability by means of ZDM of a variety of abundance structures, including (warped) rings predicted by theory, but also complex spot-like structures. Even when spectra of high signal-to-noise ratio are available, it can prove difficult or altogether impossible to correctly recover shapes, positions, and abundances of a mere handful of spots, notwithstanding the use of all four Stokes parameters and an exactly known field geometry; the recovery of (warped) rings can be equally challenging. Inversions of complex abundance maps that are based on just one or two spectral lines usually permit multiple solutions. It turns out that it can by no means be guaranteed that any of the regularization functions in general use for ZDM (maximum entropy or Tikhonov) will lead to a true abundance map instead of some spurious one. Attention is drawn to the need for a study that would elucidate the relation between the stratified, field-dependent abundance structures predicted by diffusion theory on the one hand, and empirical maps obtained by means of “canonical” ZDM, i.e., with mean atmospheres and unstratified abundances, on the other hand. Finally, we point out difficulties arising from the three-dimensional nature of the atomic diffusion process in magnetic ApBp star atmospheres.

Key words: line: profiles – stars: abundances – stars: atmospheres – stars: chemically peculiar – stars: magnetic field

1. INTRODUCTION

Ludendorff (1906) could hardly have imagined that his discovery of spectrum variations in the star α^2 CVn (after which a whole new class of variables was named) would lead to so many exciting observational discoveries and to great progress in the understanding of stellar atmospheres. When Belopolsky (1913) not only found changes in width and depth of the spectral lines, but also signs of line doubling, he could not have anticipated the continuing, unabated interest in α^2 CVn, which has led to no less than three major studies over the past 13 yr, Silvester et al. (2014) being the latest in the series. Babcock (1949b) and later Babcock & Burd (1952) observed a variable magnetic field in α^2 CVn that could, as in the case of a number of other magnetic stars (Babcock 1958), be interpreted in terms of the so-called oblique rotator model where the magnetic axis of the rotating star is inclined with respect to the rotational axis (Babcock 1949a). Deutsch (1956) speculated that the observed periodic spectral variations and radial velocity variations were in some way related to the magnetic field and worked out a method to map the abundances of various chemical elements. This method was applied to α^2 CVn by Pyper (1969) who derived curves of constant equivalent width of iron-peak elements and of rare-Earth elements in addition to a magnetic field geometry made up of a dipolar and a quadrupolar contribution.

This early work credibly established the oblique rotator model and made it clear that there had to be some correlation between the strong magnetic fields of a number of Ap stars and the abundance anomalies seen in the spectra. Now that full Stokes *IQUV* profiles of high signal-to-noise ratio (S/N) are available at high spectral resolution, the simultaneous determination of the horizontal abundance distributions of various chemical elements and of the magnetic field geometry have become feasible (see for instance the study of α^2 CVn by

Silvester et al. 2014). Claims concerning the detection of vertical stratifications of chemical elements in the atmospheres of ApBp peculiar stars have been around for quite a while—see the review by Ryabchikova (2008)—but combined maps of horizontal and vertical element distributions in conjunction with empirical magnetic geometries have not yet appeared in the literature.

Regarding theory, the idea of atomic diffusion driven by radiative accelerations being responsible for the abundance anomalies found in ApBp stars is due to Michaud (1970). The role of magnetic fields has first been explored by Vauclair et al. (1979) who demonstrated the important effect of horizontal magnetic field lines on the accumulation of silicon. Much more recently, Alecian & Stift (2010), Stift & Alecian (2012), and Alecian (2015) have modeled the vertical distributions of several chemical elements in magnetic ApBp star atmospheres as a function of field angle and field strength. These theoretical predictions can be (and sometimes have been) confronted with empirical abundance maps derived with the help of Zeeman Doppler mapping (ZDM); for a very readable introduction to ZDM see Vogt et al. (1987). Generally, these comparisons have not resulted in agreement between theory-based predictions and the detailed surface abundance distributions of a given star. Whereas Alecian (2015) has presented a thorough discussion of the limitations to the current modeling of atomic diffusion, a similar critical assessment of ZDM and the ability of its algorithms to detect complex abundance structures, in particular those predicted by diffusion theory, has not yet been undertaken.

There is thus a definite need to throw new light on this long-standing problem. In Section 2 references are given to papers presenting the techniques and algorithms underlying ZDM together with test results and there is one example of a major difference between theoretical predictions and empirical

results. A new ZDM code COSSAMDOPPLER is introduced in Section 3 and successfully subjected to tests similar to those carried out on other inversion codes. In Section 4, we show that zero-field inversions of stars with strong magnetic fields will result in spurious maps. Assuming for our tests that *all* stellar parameters are perfectly known, from atmosphere, inclination, and rotational velocity to the *exact* magnetic field geometry, and using zero-noise spectra throughout makes it possible to deal exclusively with the problem of the determination of horizontal abundance distributions and to avoid interference from other unknown stellar parameters. Section 5 deals with the uncertainties in the maps recovered with one or two lines only: many solutions turn out to be non-unique, even with all four Stokes parameters modeled to a high degree of accuracy. Theoretical results, which indicate that abundance stratifications depend on size and direction of the local magnetic field vector, are shortly discussed in Section 6, including the detectability of the predicted (warped) rings. Three-dimensional (3D) effects discussed in Section 7 introduce further complications to the modeling of magnetic Ap/Bp star atmospheres and to the interpretation of ZDM results. From the assembled evidence found in a number of Doppler maps and in view of the greatly simplified physical assumptions underlying ZDM—e.g., unstratified mean atmospheres—we conclude that the discrepancies between ZDM abundance maps and theoretical predictions often reflect shortcomings of ZDM rather than gaps in the understanding of diffusion theory.

2. ZDM, DOPPLER MAPS, AND THEORETICAL PREDICTIONS

ZDM has established itself over the last decades as a popular and apparently successful method for the mapping of stellar surface magnetic fields and of the abundance anomalies found in magnetic stars. It is still worthwhile to peruse Vogt et al. (1987) for a description of this method as applied to abundance mapping of non-magnetic stars. To constrain the ill-posed inversion problem, Vogt et al. (1987) imposed the condition that the resulting map show maximum entropy, whereas Piskunov & Kochukhov (2002) and Kochukhov & Piskunov (2002) adopted Tikhonov regularization. According to Piskunov (2001), the exact form of the regularization function is, however, not important when there are sufficient observational data with small errors. Since that time, many magnetic Ap stars have been analyzed by means of ZDM; wherever Stokes V profiles were available, or ideally the complete Stokes QUV polarized profiles, magnetic maps could be added to the abundance maps. Please note that in *all* ZDM analyses published so far, both overabundances (even the most extreme ones) and underabundances are assumed to remain constant throughout the atmosphere; in other words, stratified abundances have not been considered.

As it turns out, virtually all the published results of ZDM are at variance with the predictions of numerical diffusion models, whether based on equilibrium stratifications or on stationary solutions of the time-dependent case. Take an example: from the calculations of Alecian (2015) we expect for example Ni to behave very much like Fe. The respective maps derived for HD 50773 by Lüftinger et al. (2010a), however, differ considerably between each other, with a contrast in Ni of only 0.5 dex and a contrast in Fe of 3.4 dex. An overabundant Fe region stretches almost all around the stellar equator (similar to

Cr), whereas Ni is concentrated in two spots near the magnetic equator.

There is thus a good case for having a close look at *both* diffusion theory and ZDM in order to reach an understanding of the reasons for the apparent general disagreement. Let us make it absolutely clear that it will in no way be a goal of this paper to look at the problem of recovering magnetic field geometries. The focus is exclusively on the recovery of arbitrary abundance distributions. In this context, “arbitrary” means that abundance inhomogeneities need not necessarily take the shape of spots, and that they will in general not be “monolithic,” i.e., with a constant abundance all over the structure/spot. Keep in mind that all the tests concerning abundance inhomogeneities to be found in the literature on ZDM are based on the detection of simple “monolithic” and mostly symmetric abundance spots.

3. AN EXTENSIVELY TESTED INVERSION CODE

To demonstrate the excellent capabilities of the new COSSAMDOPPLER ZDM code we chose the abundance distribution adopted by Kochukhov (2014a, p. 6), consisting of four well-distributed “monolithic” (structureless) high-contrast spots of 20° radius. We adopted the same inclination, the same rotational velocity, the same 20 equidistant phases, and the same spectral resolution as in Kochukhov (2014a), using the single Fe II line at 4923.93 \AA . COSSAMDOPPLER uses maximum entropy regularization and finds the final abundance maps by a gradient search combined with Ng acceleration (Ng 1974). Figure 1 shows an equal-area Hammer projection of both the initial map (a) and the result of the inversion (b); as stated above, the magnetic field geometry, the inclination, and the atmospheric model were assumed to be *exactly* known. There can be no doubt that the algorithm works perfectly well and that the results compare most favorably to those shown in Kochukhov (2014a). In the inversion, all four spots are well recovered as to the positions, even the southernmost spot. For two spots, the derived maximum abundances are close to the input data, for the outlying spots near the north pole and south of the equator the abundances are less in agreement. A certain amount of smearing of the contours of the spots is visible in Figure 1, combined with extensions of the spots toward the southern hemisphere. This is a well-known effect readily discernible in Figures 5 and 9 of Kochukhov & Piskunov (2002), even more clearly so in Kochukhov (2014b, p. 40) and likewise in Kochukhov (2014a, p. 6).

COSSAMDOPPLER was also successfully applied to the Kochukhov & Piskunov (2002) test case (three spots). using the same two Fe II lines at $\lambda 6147.74$ and $\lambda 6149.26$. Thanks to hundreds of further tests with a large number of different horizontal abundance distributions, a couple of inclinations, various magnetic field geometries, and line lists containing from 1 to 20 lines, COSSAMDOPPLER certainly rivals other ZDM code as to the variety and complexity of the test abundance maps that have been inverted. More or less sophisticated magnetic field geometries adopted in our tests are only of some interest when they provide additional information on the abundances via the QUV profiles since we always assume the magnetic field to be exactly known. Let us emphasize that we have also extensively looked at spots featuring *underabundances*.

It cannot be stressed enough that the correct algorithmic working of COSSAMDOPPLER or of any other ZDM code does

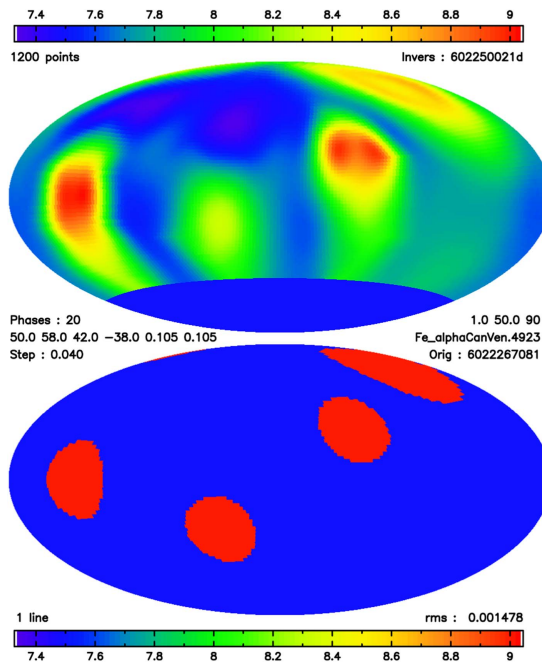


Figure 1. Equal-area Hammer projection of a four-spot Doppler mapping test case. The bottom part of the plot shows the adopted spot distribution and contrast, and the upper part is the result of the ZDM inversion. The spectral line used is the Fe II λ 4923.93 line at 20 equidistant rotational phases; the spectral resolution is 50 mÅ, giving an overall 1200 zero-noise “observational” points to be used in the inversion. The inclination i of the rotational axis is 50° , the magnetic field originating from a tilted eccentric dipole is characterized by an obliquity of $46^\circ.3$ and by a displacement from the center of 0.148 (in units of radius). The rotational velocity is 50 km s^{-1} . All stellar and magnetic field parameters are assumed to be exactly known for ZDM. The residual rms error of the fit to the line profiles points is $1.5 \cdot 10^{-3}$. Note: Hammer projections show the whole stellar surface from -90° to $+90^\circ$; the part invisible to the observer is clearly marked in the upper panel.

not imply that it has to recover—even in the most approximate way—arbitrary input horizontal abundance distributions. As long as there is no mathematical proof that with all four Stokes parameters and high S/N spectra one will invariably and of necessity correctly recover any complex abundance distribution, the only behavior that is required for a ZDM code is the proper convergence toward a good fit to the “observed” profiles and the smoothest abundance structure compatible with the data, quantified either by maximum entropy or by Tikhonov regularization. In Figures 1 and 4(c) we show that COSSAM-DOPPLER meets these requirements. If a well-tested ZDM code fails in several instances to recover the correct abundance maps, this would not automatically imply that a fundamental flaw in the ZDM algorithm had been laid bare; it could simply mean that the inverse problem at hand permits multiple solutions.

4. NEGLECTING STRONG MAGNETIC FIELDS

Stift (1996) showed that in ZDM, the adoption of an incorrect magnetic field geometry leads to spurious abundance structure, even more so when the field is neglected altogether. May we recall that the resulting horizontally non-homogeneous abundances are due to the effect of “magnetic intensification” (Stift & Leone 2003)—i.e., the splitting and ensuing desaturation of the spectral lines—but that these abundances are not directly related to the magnetic field strength and/or orientation. Rather they represent the unpredictable (because entirely

unphysical) response of the regularization function to the Zeeman splitting and the local line profiles.

With COSSAM-DOPPLER and with computing power vastly superior to what was available two decades ago, we decided to look again at the problem of zero-field inversions, and to illustrate the amazing plethora of apparent abundance structure that emerges—when the magnetic field is neglected—from Doppler mapping of a star featuring no spots. For this purpose, we have chosen the well-established field geometry of HD 154708 (Stift et al. 2013), eschewing possible criticism of using unrealistic magnetic parameters not to be found in a real star. Line profiles of four iron lines with different Zeeman patterns have been calculated for various field strengths and rotational velocities, but always with strictly the same geometry (for the definition of the non-axisymmetric tilted eccentric dipole model see Stift 1975) assuming a homogeneous iron abundance of $[\text{Fe}] = 8.00$ (on a scale with $[\text{H}] = 12.00$).

Figure 2(a) shows the abundance map obtained from the Fe II λ 4128.748 line which splits into 12 sub-components, synthesized with $v \sin i = 17 \text{ km s}^{-1}$ and a field ranging from 335 to 1290 G resulting from a tilted dipole with $48^\circ.3$ obliquity and an offset of 0.148 (in units of radius) from the center of the star. The angle between line of sight and the rotational axis is $i = 60^\circ$. As explained above, it is the regularization function that forces moderate underabundances near one pole and moderate overabundances (both about 0.2 dex) toward the equator. The fit to the “observed” profiles can be considered perfect (rms scatter of $3.5 \cdot 10^{-5}$), much better than what one could ever hope to achieve with real spectra. A somewhat different map (b) is obtained from the Fe II λ 4177.692 line, split into 18 Zeeman sub-components, with the field almost three times larger than in the previous case, but with the same magnetic geometry. The star rotates at $v \sin i = 24 \text{ km s}^{-1}$ and the inclination is $i = 75^\circ$. The respective extensions and structures of the spots have changed and the range in spurious abundances is substantially larger than before, ranging from 7.91 to 8.56. Most disturbingly, exactly the same field strength and magnetic geometry lead to still another map (c) when the inversion is based on the Fe II λ 4258.154 line split into 10 sub-components, with inclination $i = 60^\circ$ and rotational velocity $v \sin i = 35 \text{ km s}^{-1}$. Substantial overabundances are found all over the star, ranging from 0.5 to 1.2 dex. That the trend with magnetic field strength is entirely unpredictable becomes obvious from the map at the top (d). For this particular simple Zeeman triplet (Fe I λ 4063.594), with $i = 55^\circ$ and $v \sin i = 45 \text{ km s}^{-1}$, the spurious spots reach a contrast of more than 0.5 dex, the apparent overabundances attain 0.8 dex and the map again changes substantially. It has to be stressed that in all four examples shown, the fits to the “observed” profiles can for all practical purposes be considered perfect.

Let us illustrate with the neutral oxygen triplet $\lambda\lambda$ 7771.941, 7774.161, 7775.390 why zero-field inversions of the spectra of strongly magnetic stars like HD 3980 (Nesvacil et al. 2012) yield spurious horizontal abundance structure. For a field strength of $B = 7 \text{ kG}$ Zeeman splittings become quite large, viz. 0.265, 0.377, and 0.346 Å for effective Landé factors of 1.34, 1.91, and 1.75, respectively. At a given wavelength, intensity values can differ hugely between the unsplit lines and the Zeeman-split lines. In the longitudinal field case, intensities at the respective positions of the unperturbed lines attain a level very close to the continuum. Conversely, at $\pm 10.2 \text{ km s}^{-1}$ from the center of the λ 7771.941 line—where normally the line disappears in the

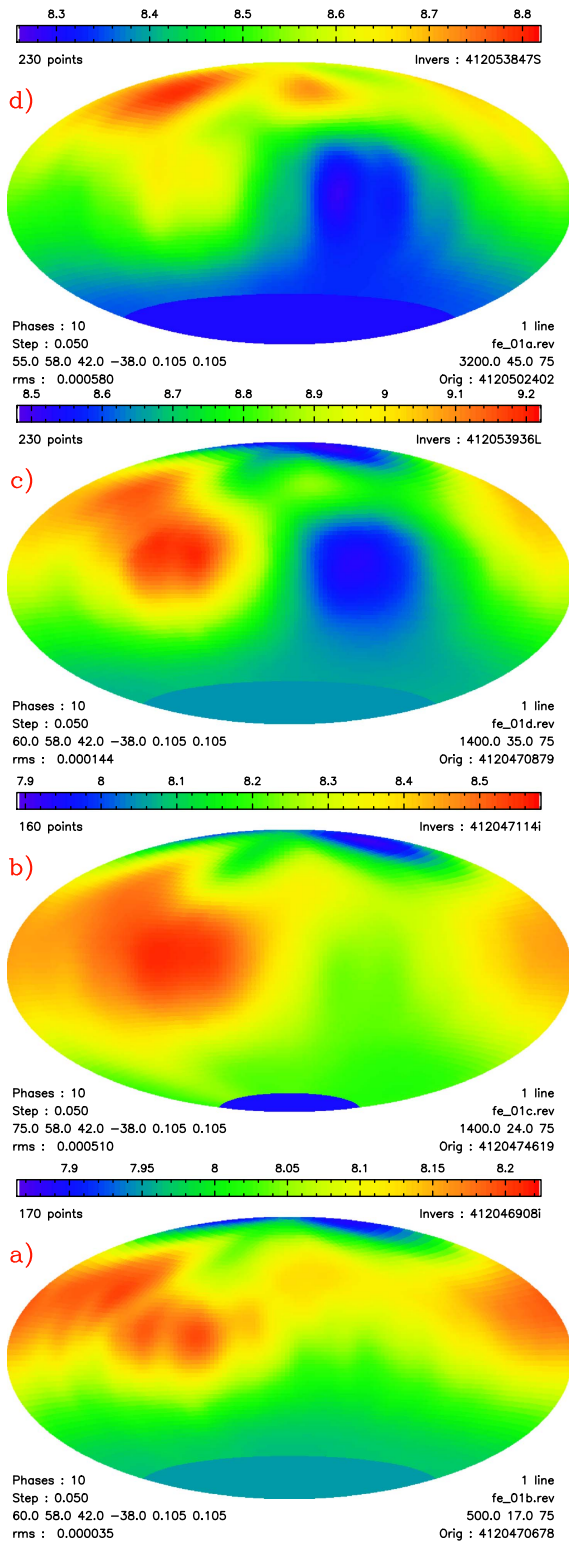


Figure 2. Spurious ZDM maps obtained by neglecting the magnetic field of stars featuring no spots. The magnetic geometry adopted for calculating the “observed” profiles is the same for all four plots; field strength, inclination, and rotational velocity differ as do the Zeeman splittings of the lines used.

continuum—opacity from the σ -components reaches its maximum. The splitting of the outermost σ -component corresponds to $\pm 17.8 \text{ km s}^{-1}$. The lines making up the triplet all exhibit different Zeeman patterns. Maximum opacity of the σ -components is found at $\pm 14.6 \text{ km s}^{-1}$ for the $\lambda 7774.161$ line, and

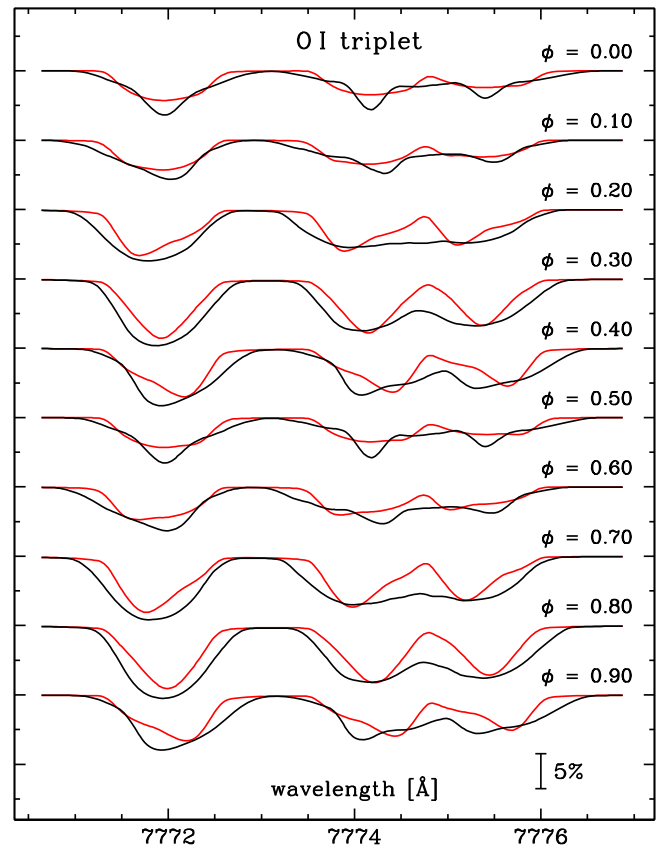


Figure 3. Predicted phase-dependent profiles of the oxygen triplet for a spot distribution very similar to that claimed for HD 3980 by Nesvacil et al. (2012). The profiles in black have been calculated with the magnetic field postulated by Nesvacil et al. (2012) with a polar field strength of $B_p = 7 \text{ kG}$. The red profiles pertain to a zero-field synthesis.

at $\pm 13.3 \text{ km s}^{-1}$ for the $\lambda 7775.390$ line. The splitting of the outermost σ -component of the latter transition corresponds to $\pm 19.1 \text{ km s}^{-1}$, which has to be put in relation to the rotational velocity ($v \sin i = 22.5 \text{ km s}^{-1}$ for HD 3980). In a zero-field inversion, the Doppler mapping algorithm must interpret the missing signal from the line center as a sign of an extremely low abundance, the signal from the σ -components as coming from spots, even when real abundance spots are absent. Confusingly enough, the respective signals from the apparent spots would show up at different positions for the three lines.

It is instructive to model the spectrum variations resulting from two major oxygen abundance spots (see Figure 4 of Nesvacil et al. (2012)) with their suggested dipole field and without it. The results displayed in Figure 3 reveal that over the majority of phases, large discrepancies exist between magnetic and non-magnetic profiles. This clearly shows that non-magnetic Doppler mapping of strongly Zeeman-split spectral lines cannot recover the true horizontal abundance maps.

5. IN A SINGLE LINE WE TRUST?

Even a cursory survey of the relevant literature brings to light a large number of inversions based on a mere one or two spectral lines. In all, at least 35 maps have been published that have been derived from one line only of the element in question; at least 22 more Doppler maps rely on the analysis of two lines. What about the reliability of these single-line or double-line inversions? To investigate this question we decided

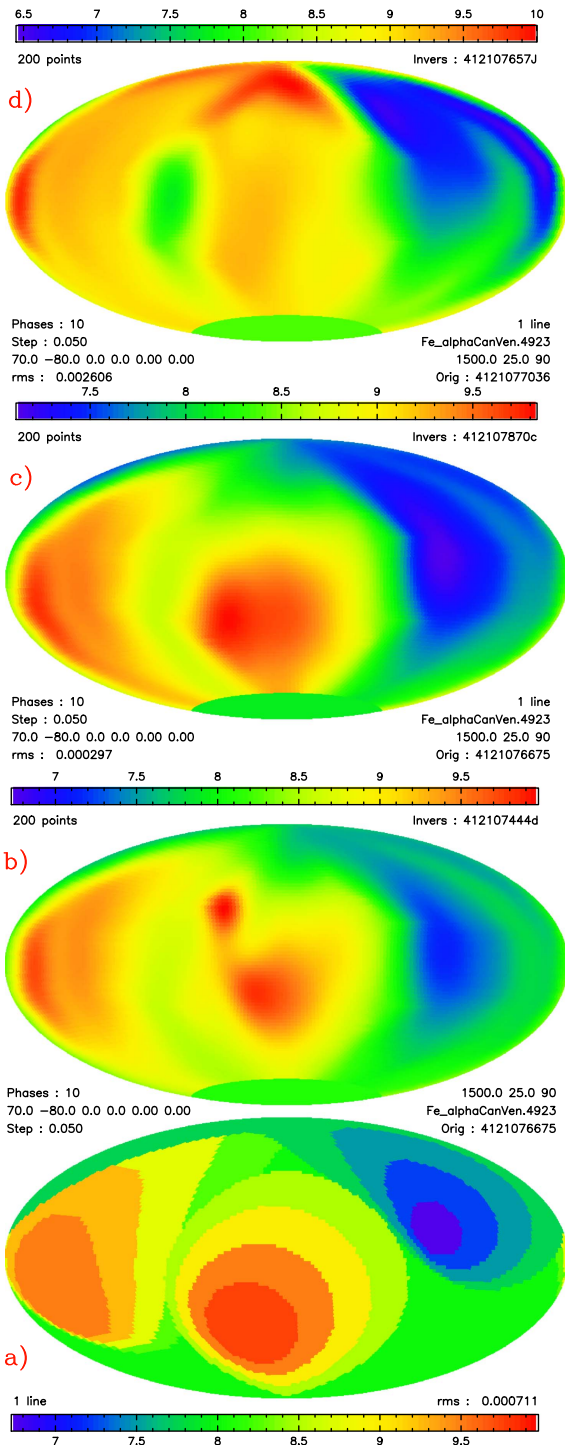


Figure 4. ZDM maps from inversions based on the Fe II $\lambda 4923.93$ line (50 mÅ resolution, $i = 70^\circ$, $v \sin i = 25 \text{ km s}^{-1}$, centered dipole with 80° obliquity, polar field strength $B_p = 3 \text{ kG}$). At the bottom (a) we show the adopted distribution of three large spots with inner structure, the map just above (b) gives the result of an inversion based on Stokes I only. Map (c) results from an inversion with all four Stokes $IQUV$ parameters. When the phase-dependent spectra are calculated with the correct local atmospheres, but a constant mean atmosphere all over the star is adopted in the inversion, we get the map displayed at the top (d).

to consider lines from several different Fe line lists, among them the lists published by Kochukhov & Wade (2010) and by Kochukhov et al. (2004).

Figure 4(a) shows a fairly simple configuration of three extended spots: in two spots, abundances increase toward the

center, in one spot the abundance decreases. Using only the Stokes I profile of the Fe II $\lambda 4923.93$ line—employed in the mapping of $\alpha^2\text{CVn}$ —one obtains a map that can hardly be called a full success (b). Even though the three spots are recovered in some approximate form, shapes and positions relate rather poorly to those of the input model. Map (c), based on all four Stokes parameters, seems much more satisfactory, but still does not take into account the fact that the local atmosphere changes substantially with metal abundances—in particular of Fe and Cr—as pointed out by Stift et al. (2012). When the phase-dependent spectra are correctly calculated with the appropriate local atmospheres, and when in the inversion a constant mean atmosphere all over the star is adopted (as in essentially all inversions published so far) we arrive at the map shown at the top (d). This map bears very little resemblance to the original input map; the central strong spot disappears and one finds a strange high-abundance feature emerging near the northern pole.

Finally, we looked at a considerably more complex abundance map consisting of five spots and one ring-like structure (Figure 5). The Stokes I only inversion with the Fe II $\lambda 4923.93$ line fails completely, recovering just the position of the central spot. Adding the $\lambda 5018.44$ and using all four Stokes parameters, the number of available profile points to be fitted is multiplied by a factor of eight but to no avail. The map only changes a wee little bit and still no more than one or two of the six abundance structures in the input model can be approximately recovered! Once again we point out the excellent fit to the “observed” Stokes profiles of both the Fe II $\lambda 4923.93$ and the $\lambda 5018.44$ lines, with an rms scatter of $6.6 \cdot 10^{-4}$. Just think what happens when real stellar spectra are inverted: there is absolutely no way to ascertain the nature of the resulting maps, whether they represent the true horizontal abundance inhomogeneities or whether they are spurious. The decisive criterion is the best fit to the data, subject to the restrictions imposed by the adopted regularization function. Whoever obtains results as displayed in Figure 6 from an unknown stellar source will not hesitate to accept this solution. To put it succinctly: the fact that two completely different abundance maps lead to the same perfect fit to all four noise-free Stokes profiles of two unblended spectral lines (with precisely known atomic parameters) in a star with exactly known physical parameters and exactly known magnetic geometry unequivocally demonstrates the existence of multiple solutions to the ZDM problem.

6. ENTER DIFFUSION THEORY

The statement that appropriate local atmospheres have to be used in the proper modeling of magnetic Ap stars with pronounced horizontal abundance inhomogeneities has to be elaborated upon in view of the results on atomic diffusion in magnetic fields presented by Alecian (2015). Looking at the literature on Ap stars we find what amounts to a tacit agreement on a spot-stratification dichotomy. In ZDM, abundances (and magnetic fields) are allowed to vary horizontally, but are assumed—at a given point on the surface—to be vertically constant from the bottom to the top of the atmosphere. Conversely, in the abundance analysis of stars like γEqu or βCrB , the assumed absence of spots is accompanied by stratification profiles that are constant all over the star, regardless of the local magnetic field vector. One of the few examples of a star having been subjected to analyses according

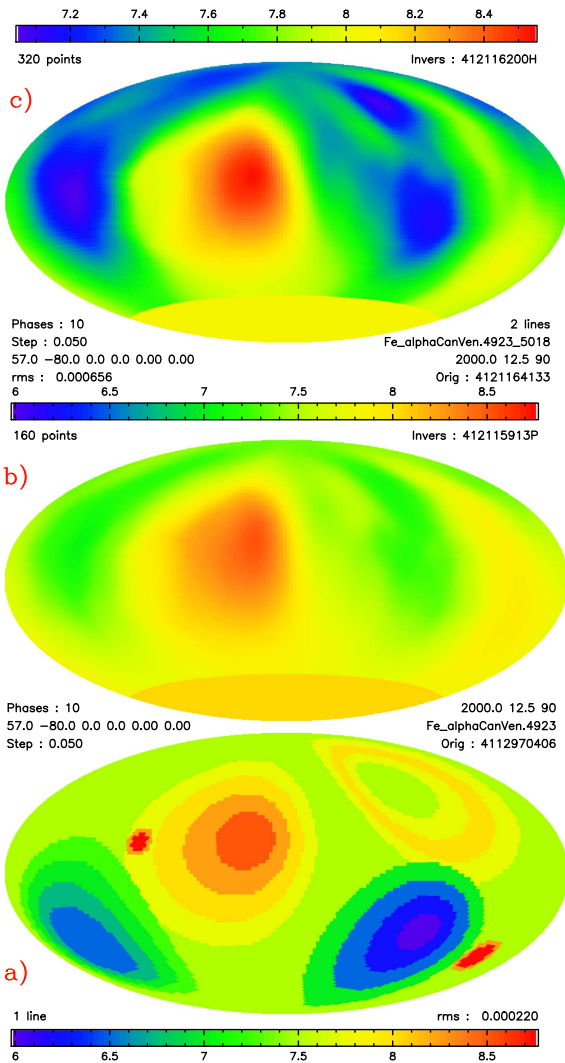


Figure 5. ZDM maps from inversions based on the Fe II λ 4923.93 and λ 5018.44 lines. At the bottom (a) we show the adopted abundance distribution characterized by one ring-like feature and five spots of varying extension and structure. The map just above (b) gives the map based on the Stokes I profiles of λ 4923.93 only. The top map (c) results from an inversion using all four Stokes $IQUV$ parameters of both Fe II lines.

to both these scenarios is HD 24712; Lüftinger et al. (2004) found a 2 dex jump in the *global vertical* Fe distribution, whereas the *horizontal* contrast in the unstratified ZDM analysis by Lüftinger et al. (2010b) is limited to about 0.6 dex. Underabundances relative to the solar value range from -0.1 dex to -0.7 dex. Can these apparently conflicting results be explained within the framework of diffusion theory? Attention should be drawn to a caveat in the paper by Lüftinger et al. (2010b). It says: “It is still possible however that part of the horizontal abundance structure we find is due to variation of the chemical stratification profile across the stellar surface.” In fact, variations in the stratification profiles are exactly what the time-dependent simulations of the diffusion of iron-peak elements predict. Figures 3 and 5 of Stift & Alecian (2016) reveal a strong dependence of the Fe stratification on the angle of the magnetic field with respect to the surface normal, to a substantially lesser degree on the magnetic field strength.

So far, the literature on ZDM has dealt almost exclusively with the detection of spot-like abundance structures. For this

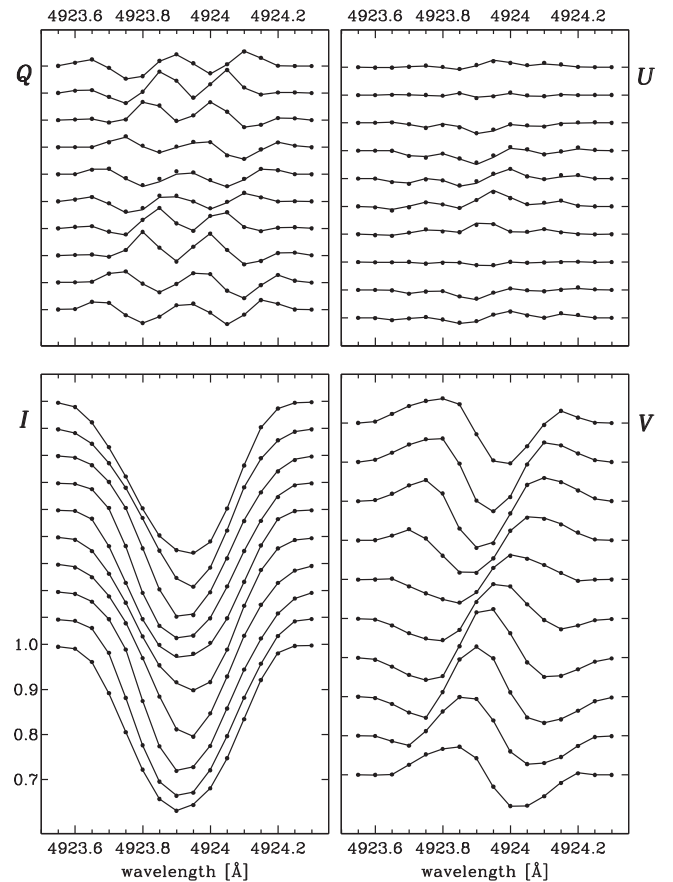


Figure 6. Fit to Stokes $IQUV$ profile variations of the Fe II λ 4923.93 line. The filled circles have been calculated with the surface abundance structure displayed in Figure 5(a), and the lines represent the best fit to these “observed” profiles and are based on the abundance map shown in Figure 5(c). The latter map is clearly characterized by a higher entropy than the original map. The profiles are offset by 6% in I , 3% in Q and U , and by 8% in V .

kind of structure, it has been established in the preceding sections that abundance maps obtained by zero-field inversions of stars with fields of several kG can in no way be relied upon; single-line inversions often permit multiple solutions. There can hardly be any doubt that these findings continue to hold true for the rings about the magnetic equator predicted by Alecian & Stift (2010). What is less clear is the answer to the question of how well ring-like abundance structures can be recovered once the magnetic field geometry, the field strength, and the angle between rotational axis and the observer are all exactly known as in our previous discussion. In that context one has to be aware of the fact that the rings resulting from magnetic surface fields represented by the non-axisymmetric eccentric tilted dipole model will in general be warped. For a successful application of the eccentric tilted dipole to β CrB and to HD 126515, see Stift (1975) and Stift & Goossens (1991); HD 154708 has been the object of a more sophisticated study including the modeling of the profiles of near-infrared lines of Si (Stift et al. 2013).

To start with a simple idealized case, we assumed the magnetic geometry of HD 154708 and vertically constant overabundances at the magnetic equator, decreasing rapidly with the angle between field vector and the surface normal as shown in Figure 7(a). The ZDM inversion based on the two iron lines λ 4923.93 and λ 5018.44 yields a very unsatisfactory map (b) with a single dominating spot when only Stokes I is

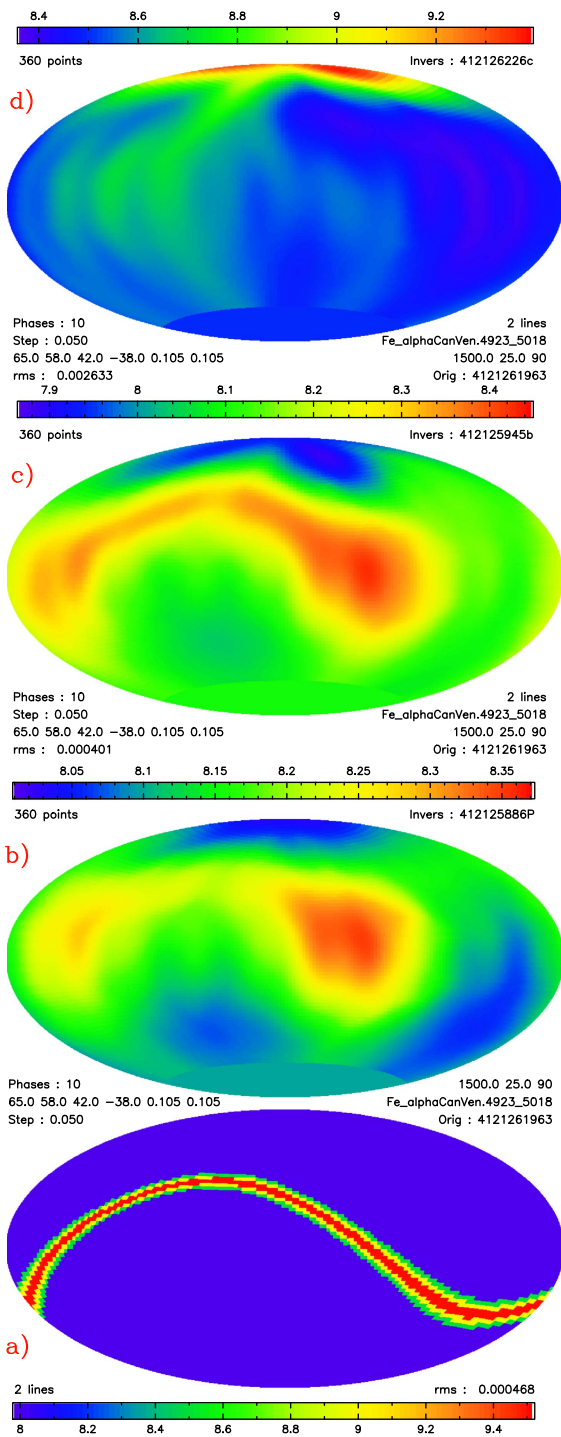


Figure 7. ZDM inversions based on the two Fe II lines at $\lambda 4923.93$ and $\lambda 5018.44$. A warped ring of enhanced abundances, which follows the magnetic equator, is shown at the bottom (a). The map just above (b) represents the ZDM result based on Stokes I profiles only. Map (c) has been derived with the help of all four Stokes parameters. In both cases the stellar and magnetic field parameters have been assumed to be exactly known. A zero-field inversion yields the perfectly spurious map at the top (d). Note the spectacular north polar spot.

used. Please note the extremely reduced contrast! With all four Stokes parameters, the inversion (c) seems to recover at least part of the ring, which, however, is very much washed out, still suffers from a highly reduced contrast, and looks rather like two spots connected by a kind of bridge. Near the pole there

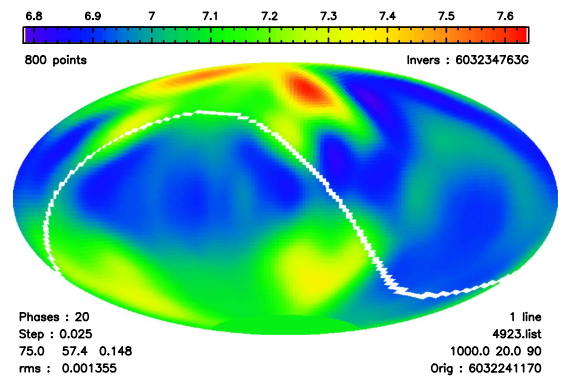


Figure 8. Doppler map obtained from the inversion of the Fe II $\lambda 4923.93$ line, adopting a mean atmosphere with $T_{\text{eff}} = 10,000$ K, $\log g = 4.0$, and $[\text{Fe}] = 8.0$. The input spectrum has been calculated with field-dependent stratification profiles as shown in Stift & Alecian (2016); overabundances decrease with distance from the magnetic equator (indicated as a white warped ring). The non-axisymmetric oblique rotator model is characterized by inclination $i = 75^\circ$, obliquity $\beta = 57.4$, and dipole offset 0.148 (in units of stellar radius). Field strengths range from 660 to 2375 G.

now appears a region exhibiting what looks like moderate underabundances. Finally we establish an entirely spurious map (d) by carrying out a zero-field inversion with the two lines given above. A spectacular north polar spot emerges with some wispy structure extending toward the southern pole. In contrast to the inversions where the magnetic field has been fully taken into account, the fit to the profiles is no longer perfect but definitively not worse than what has been achieved for HD 3980 by Nesvacil et al. (2012). The present idealized examples indicate that seemingly simple warped abundance rings can be difficult to recover (as are multiple spots as shown before) despite an exact knowledge of the magnetic field strength and geometry, particularly if the inversion relies on just one or two lines and if only Stokes I is used. The probability of obtaining the true abundance maps appears to increase with the use of all four Stokes parameters but even then it cannot be excluded that the inversion results in a spurious map.

The physical reality that emerges from time-dependent diffusion calculations makes ZDM analyses even more difficult, almost intractable. The abundances still depend on the angle between magnetic field vector and surface normal but they can no longer be considered constant with depth. Abundances are stratified, stratification profiles change with angle, overabundances in the higher layers of the atmosphere can be accompanied by underabundances in intermediate layers. So far this has not been taken into account in any of the numerous ZDM inversions, mean unstratified atmospheres being at the basis of every map published. In order to reveal the repercussions of these changing stratification profiles on ZDM results, we decided to synthesize a spectrum resulting from detailed theoretical field-dependent stratifications and to carry out an inversion with a mean unstratified atmosphere. We selected the Fe II $\lambda 4923.93$ line and we chose a magnetic geometry similar to the one determined for HD 154708. The resulting abundance map, based on a fit to all four Stokes parameters and with the effect of the magnetic field taken correctly into account, is shown in Figure 8. For illustrative purposes, the magnetic equator is outlined. The plot makes it abundantly clear that the intrinsic correlation between magnetic field direction and abundances is not recovered.

7. CAVEATS AND CONCLUSIONS

There is an apparent contradiction between theoretical models and the ever increasing number of (Zeeman) Doppler maps that have accumulated over recent years. Although this unsatisfactory situation has consistently been imputed to theory, there are good reasons to question the validity of the assumptions underlying the interpretation of ZDM results, viz., that abundances are unstratified, that mean stellar atmospheres are a good approximation to the local atmospheres, and that abundance maps are unique. We do not pretend that the present-day status of diffusion theory and associated numerical modeling are unassailable or that the world is near to a reasonably full understanding of what happens in the atmospheres of magnetic ApBp stars. However, we think that any valid criticism of theoretical work on diffusion that argues with contrasting empirical results needs to be based on extensive and realistic tests. Such tests have to involve all well-known stellar atmospheric physics (e.g., the metallicity dependence of the temperature and pressure structure), they must not be restricted to spot-like abundance structures, and they have to include stratification of the chemical elements—which are both predicted by theory and detected in stellar spectra. Only when it can be shown that ZDM is capable of recovering combined vertical and horizontal complex abundance structures will the confrontation between theory and ZDM maps lead to progress in the understanding of the physics ApBp stars.

This paper finally partially remedies this situation by demonstrating unequivocally that even in fairly simple test cases, be they based on three to seven spots that are not assumed monolithic, or on a warped ring following the magnetic equator in a tilted eccentric dipole model, there is no guarantee whatsoever that the surface abundance structure taken for input will be correctly recovered. This holds in particular for inversions using only a single spectral line in Stokes I , but unexpectedly, even with all four Stokes $IQUV$ parameters and/or more lines, a completely spurious abundance map can by no means be excluded. This comes somewhat as a surprise since in our tests we have always assumed the magnetic field strength and geometry to be *exactly* known (zero-field inversions of course excepted) and the dependence of the local atmosphere on the abundance—taken to be vertically constant—to be negligible. Any abundance map derived from only one or two lines must therefore be regarded with suspicion. Let us finally repeat that the application of zero-field inversions to strongly magnetic stars cannot give correct results; overabundances of manganese and oxygen (claimed to be as abundant as He), or of Si, which allegedly is as abundant as hydrogen, must be considered spurious and unphysical as will be shown below.

7.1. A Bleak Outlook?

From the results discussed in the preceding sections it has emerged that ZDM has so far failed to provide us with really trustworthy empirical data that could serve as constraints to theory. It is also true that at present numerical modeling of atomic diffusion is not capable of predicting abundance maps and stratifications for a given star. It has been established, however, that the build-up of vertical abundance structure is highly sensitive to the inclination of the magnetic field lines (see e.g., Stift & Alecian 2016). Since both equilibrium and time-dependent stationary stratifications have been found to

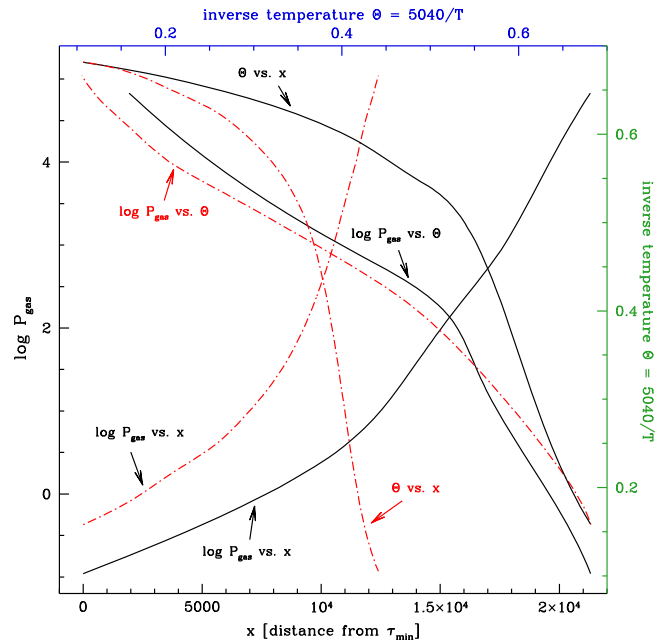


Figure 9. Structure of two stellar atmospheres with identical $T_{\text{eff}} = 12,000$ K and $\log g = 4.0$, but different Fe abundances. The black full lines show the results for $[\text{Fe}] = 7.50$; the dash-dotted red lines for $[\text{Fe}] = 10.50$. The abundances of all other 91 elements are assumed to be solar.

depend strongly on the field direction, it becomes clear that ZDM analyses based on mean unstratified atmospheres and localized vertically constant over- and/or underabundances are inadequate; the same holds for stratification analyses that assume the same vertical abundance profile all over the star.

There are more fundamental problems looming beyond the horizon of these field-dependent stratifications. On the theoretical side, it appears impossible to determine stratifications in magnetic ApBp atmospheres by means of a two-dimensional approach, i.e., by approximating them by isolated “cylinders” characterized by specific stratification profiles of the various elements and the corresponding local atmosphere. Let us outline the basic arguments for this pessimistic assessment by looking at the mean molecular weight of the gas. For solar abundances, we have approximately $\mu = 1.26$. Taking the abundance values shown in Figures 4–6 of Nesvacil et al. (2012), this becomes something like $\mu = 16$, more than 10 times the solar value. The local pressure scale height inside the spot would therefore be just 1/12 of the scale height of the surroundings. In order to visualize the kind of problem arising from such a configuration, we calculate model atmospheres corresponding to the “normal” atmosphere and to the spot with the extreme abundances. Since it defies the capabilities of the Atlas family of codes to establish atmospheres with excessively high abundances, we restrict ourselves to the case of $[\text{Fe}] = 10.50$, with the other elements exhibiting solar abundances, resulting in $\mu = 2.8$. Figure 9 reveals the huge differences—which reach several orders of magnitude—in gas pressure at a given geometrical depth x (counted from the respective minimum optical depths of the atmospheric models). The greatly reduced scale height in the spot, 45% of the scale height outside, also shows up clearly in the respective temperature versus x relations. For illustrative purposes, we have additionally plotted the relations P_{gas} versus temperature, which display noticeable differences too.

In the absence of stabilizing forces, a system consisting of a stellar spot and the “normal” atmosphere will establish horizontal pressure equilibrium on the dynamical timescale, i.e., almost instantaneously with respect to the slow diffusive motions that lead to the build-up of vertical abundance inhomogeneities. Pressure differences will swiftly be ironed out by horizontal flows of material. All of this admits of one conclusion only: spots with extreme unstratified overabundances, embedded in an atmosphere with very different unstratified abundances, cannot remain stable. One might object that strong vertical magnetic fields could stabilize the high-abundance “cylinders,” but this is not likely to work. Take for example observational evidence from 53 Cam and the stunning complexity of its magnetic field (Piskunov 2008) with field strengths ranging from 1.4 to 26.1 kG. The abundances and positions of the Fe spots with respect to the magnetic field defy simple explanations: both the largest overabundance and the most extreme underabundance are found at positions on the stellar disc that can be considered magnetic poles, featuring field strengths in excess of 20 kG. The spot with the second-largest Fe overabundance is located near the magnetic equator and there is no vertical field either to confine the strong Si spots, which are situated near the magnetic equator. How could one ever reconcile such strange spot behavior with a stabilizing magnetic field?

Observationally, one has to realize that there would be a much larger number of free parameters to be determined with the help of ZDM than generally assumed. Instead of having to deal with a single abundance value for every surface element, an entire stratification profile has to be determined, which in turn depends not only on the magnetic field strength and direction at a particular position, but also on the respective magnetic geometries of all the surrounding surface elements. Donati, in 2001 at the conference on “Magnetic Fields Across the Hertzsprung–Russell Diagram,” surmised that irrespective of the regularization function used, data sets with all four Stokes parameters did not necessarily contain enough information on the field to accurately recover the magnetic distribution (even in simple cases) and advocated the introduction of physical constraints that could possibly remove the indeterminacy of the ill-posed inverse problem. It is to be feared that physical constraints will be difficult or even impossible to establish. Certainly it is feasible to apply a truly multi-line approach with spectral lines that exhibit very different center-to-limb behavior as presented in Figure 3 of Stift (1986) in order to maximize the diagnostic content of the simultaneously modeled separate Stokes *IQUV* profiles. One can also certainly afford to establish appropriate stratified local atmospheres so that there is no need to base inversion codes on mean atmospheres. Still, even if a whole theoretical grid of individual

stratifications as a function of magnetic field angle and field strength were available, there is no way to predict and parameterize the 3D abundance structure of an ApBp star permeated by a non-axisymmetric magnetic field with a warped magnetic equator.

Thanks go to Ivan Hubeny for most helpful discussions.

REFERENCES

- Alecian, G. 2015, *MNRAS*, **454**, 3143
Alecian, G., & Stift, M. J. 2010, *A&A*, **516**, A53
Babcock, H. W. 1949a, *Obs*, **69**, 191
Babcock, H. W. 1949b, *PASP*, **61**, 226
Babcock, H. W. 1958, *ApJ*, **128**, 228
Babcock, H. W., & Burd, S. 1952, *ApJ*, **116**, 8
Belopolsky, A. 1913, *AN*, **196**, 1
Deutsch, A. J. 1956, *PASP*, **68**, 92
Kochukhov, O. 2014a, Exercise: Surface Cartography of the Sun and Stars, Besançon
Kochukhov, O. 2014b, Lecture: Surface Cartography of the Sun and stars, Besançon
Kochukhov, O., Bagnulo, S., Wade, G. A., et al. 2004, *A&A*, **414**, 613
Kochukhov, O., & Piskunov, N. 2002, *A&A*, **388**, 868
Kochukhov, O., & Wade, G. A. 2010, *ApJ*, **513**, A13
Ludendorff, H. 1906, *AN*, **173**, 1
Lüftinger, T., Fröhlich, H.-E., Weiss, W. W., et al. 2010a, *A&A*, **509**, A43
Lüftinger, T., Kochukhov, O., Ryabchikova, T., et al. 2010b, *A&A*, **509**, A71
Lüftinger, T., Kochukhov, O., Ryabchikova, T., Ilyin, I., & Weiss, W. W. 2004, in *IAU Symp. 224, The A-Star Puzzle*, ed. J. Zverko et al. (Cambridge: Cambridge Univ. Press), 253
Michaud, G. 1970, *ApJ*, **160**, 641
Nesvacil, N., Lüftinger, T., Shulyak, D., et al. 2012, *A&A*, **537**, A151
Ng, K.-C. 1974, *JChPh*, **61**, 2680
Piskunov, N. 2001, in *ASP Conf. Ser. 248, Magnetic Fields Across the Hertzsprung–Russell Diagram*, ed. G. Mathys, S. K. Solanki, & D. T. Wickramasinghe (San Francisco, CA: ASP), 293
Piskunov, N. 2008, *PhST*, **133**, 014017
Piskunov, N., & Kochukhov, O. 2002, *A&A*, **381**, 736
Pyper, D. M. 1969, *ApJS*, **18**, 347
Ryabchikova, T. 2008, *CoSka*, **38**, 257
Silvester, J., Kochukhov, O., & Wade, G. A. 2014, *MNRAS*, **444**, 1442
Stift, M. J. 1975, *MNRAS*, **172**, 133
Stift, M. J. 1986, *MNRAS*, **221**, 499
Stift, M. J. 1996, in *IAU Symp. 176, Stellar Surface Structure*, ed. K. G. Strassmeier & J. L. Linsky (Dordrecht: Kluwer), 61
Stift, M. J., & Alecian, G. 2012, *MNRAS*, **425**, 2715
Stift, M. J., & Alecian, G. 2016, *MNRAS*, **457**, 74
Stift, M. J., & Goossens, M. 1991, *A&A*, **251**, 139
Stift, M. J., Hubrig, S., Leone, F., & Mathys, G. 2013, in *ASP Conf. Ser. 479, Progress in Physics of the Sun and Stars: A New Era in Helio- and Asteroseismology*, ed. H. Shibahashi & A. E. Lynas-Gray (San Francisco, CA: ASP), 125
Stift, M. J., & Leone, F. 2003, *A&A*, **398**, 411
Stift, M. J., Leone, F., & Cowley, C. R. 2012, *MNRAS*, **419**, 2912
Vauclair, S., Hardorp, J., & Peterson, D. M. 1979, *ApJ*, **227**, 526
Vogt, S. S., Penrod, G. D., & Hatzes, A. P. 1987, *ApJ*, **321**, 496